PRIMARY EMITTER LOCALIZATION USING SMARTLY INITIALIZED METROPOLIS-HASTINGS ALGORITHM

Suzan Üreten, Abbas Yongaçoğlu, Emil Petriu

University of Ottawa
School of Electrical Engineering and Computer Science
800 King Edward Ave. Ottawa ON K1N 6N5 Canada
E-mail: suzan.ureten@ieee.org

ABSTRACT

The knowledge of the primary emitter location is important in cognitive radio networks as it is required to determine the exclusion region of the primary network. We show that interpolation based localization techniques do not provide accurate primary emitter localization; however they can provide significant complexity reduction when their estimates are used to initialize more accurate iterative localization techniques. In this paper, we generated interference maps using low complexity interpolation techniques and provided their coarse estimates to initialize a Metropolis-Hastings (MH)based localization algorithm. Our simulation results show that smart initialization of the MH algorithm eliminates tedious parameter tuning process and achieves significantly better localization performance than randomly initialized MH algorithm at a fraction of iterations.

Index Terms— Cognitive radio networks, interference map, primary emitter localization, Markov chain Monte Carlo.

1. INTRODUCTION

The ever increasing use of wireless services is generating a spectrum shortage problem. Flexible radio technologies based on new dynamic access paradigms have been proposed to address this problem. One challenge of dynamic spectrum access is to decide whether the spectrum is available at a given location and time. The problem is complicated due to factors such as hidden nodes and sensitivity requirements.

The radio environment map (REM) concept has been introduced as a versatile tool to maintain the operation of cognitive radios. The REM contains information about the radio environment in several domains such as terrain information, radio regulations and static RF emissions. A map that displays the level of interference over the region of interest (ROI) is called an interference cartograph and it can be one of the layers of the REM [1]. An interference map can be captured by combining measurements performed by different network elements and may assist several tasks such as sensing and setting primary exclusion region. Creating an interference map requires measuring the received signal power at multiple locations in the ROI, which is impractical in dynamic scenarios where the number and locations of measurements change. However, in many applications, effective spatial interpolation techniques can be used to generate an interpolated map from a given number of sensor measurements and locations.

Several interpolation methods have been introduced for obtaining interference maps from received signal strength (RSS) measurements. The ambient RF power spectrum is regarded as a random field, and the kriging method has been used to estimate the spatial power spectral density (PSD) in [2]. Kriging has also been adopted as a reliable spatial interpolation scheme to generate an interference map [1]. An iterative REM building process based on kriging interpolation is presented in [3]. In [4], a performance comparison of kriging, spline and a local interpolation technique, namely natural neighbour interpolation, has been presented. It is shown that the natural neighbour interpolation provides a level of performance in terms of primary emitter localization and field strength estimation efficiency comparable to that of effective global techniques such as kriging. In [5], Delaunay triangulation based interpolation techniques have been considered for generating interference maps due to their convenience for distributed implementation. Local information processing techniques such as Delaunay based interpolation, require data only from the neighbouring nodes, therefore they provide advantages over the global techniques especially in ad hoc networks where the network topology is affected by the local changes for example due to mobility. In such cases it is more efficient to perform local computations rather than implementing network-wide updates. Besides, triangulation is a generic tool that serves as a basis for many geometry-based algorithms in wireless networks to enable local information processing. Therefore the use of actual triangulation provides a computationally attractive solution for the interference map generation problem.

The accuracy of emitter location estimates obtained from an interpolated interference map is usually poor compared to more sophisticated localization techniques. However, a coarse estimate obtained from the interference map can be adequate to initialize more accurate localization algorithms either to reduce computational complexity or to improve estimation accuracy. In this paper, we present a case where

the knowledge acquired from a REM is further utilized for reducing the complexity of an accurate emitter localization technique. Specifically, we consider reducing the number of iterations of the Metropolis-Hastings (MH) algorithm for emitter localization. The performance of MH algorithm is affected by several design parameters such as the selection of proposal density and its parameters, number of iterations and burn-in samples. Even though MH algorithm is guaranteed to converge, the convergence may be slow. In this work, we show that smart initialization of the MH algorithm improves the convergence dramatically.

2. PROBLEM DEFINITION

We consider a secondary radio network consisting of a number of users deployed at known locations in a given ROI. We assume that one primary user is active at any given time and each secondary user measures the received power due to the primary transmitter. In the considered scenarios, nodes are communicating with their neighbours and form an ad-hoc network. The network is assumed to be triangulated for networking tasks and the triangulation is then utilized for generating the interference map based on interpolation. The interpolation techniques considered in this paper are nearest neighbour and linear interpolation based on Delaunay triangulation[5]. The coarse estimate obtained from the interference map initializes the MH localization algorithm with the objective of reducing the number of iterations.

3. PRIMARY EMITTER LOCALIZATION

In this section, we provide a brief introduction to two different emitter localization approaches used in this paper. The first approach is based on interference maps generated using interpolation techniques whereas the second approach relies on the MH-algorithm.

3.1. Localization using interference map

An interference map indicates the level of interference in a region of interest and it can be obtained by applying simple and effective spatial interpolation techniques utilizing measured power levels from distributed sensors and their locations [1]. Using this information, a secondary network can geo-locate a primary transmitter based on the location of the maxima of the map [4],[5].

In this paper, we consider Delaunay triangulation based interpolation for generating interference maps. Delaunay triangulation is frequently used for many networking tasks such as routing and topology control and the use of existing triangulation provides a computationally attractive solution for interference map generation [5]. Among the Delaunay based interpolation techniques, linear interpolation provides a level of performance comparable to other more complex techniques such as natural, cubic and quadratic interpolations [5]. On the other hand, the nearest neighbour (NN) interpolation is the least computationally complex technique but its performance

is significantly lower than the other triangulation based techniques. In this paper, we consider linear and NN interpolations due their lower complexity.

A Delaunay triangulation for a set of given nodes is a triangulation of the set such that no node in the set is inside the circumcircle of any triangle in the triangulation. Voronoi decomposition is the dual representation of this triangulation and partitions a plane into convex polygons such that each polygon contains exactly one generating point and every point in a given polygon is closer to its generating point than to any other. The decomposition can be obtained by connecting the centres of the circumcircles of the Delaunay triangulation. In this work, the quick hull algorithm is used to construct Delaunay and Voronoi diagrams. Details of the quick hull algorithm can be found in [6].

The NN interpolation algorithm computes the interference map value at any given location based on the Voronoi decomposition; specifically all the points inside a Voronoi cell take the value of that Voronoi site. Linear interpolation algorithm computes the map value based on the triangulation; the value at a location inside a triangle is computed as a linear combination of the sensor measurement at the triangle vertices. More information about generating interference maps using the Delaunay based NN and linear interpolations and their application to primary emitter localization can be found in [5].

3.2. Localization Using MH

The Metropolis-Hastings (MH) algorithm is a Markov chain Monte Carlo method for generating a sequence of random samples from a probability distribution for which direct sampling is difficult. The general idea of the algorithm is to use a Markov chain that generates states depending on the likelihood ratio of the states. The chain starts from a random state. By using a proposal density $Q(x'; x(t))$, which depends on the current state $x(t)$, a new proposed sample x' is generated. This proposal is accepted as the next value by checking the acceptance ratio $\eta = \min(1, P(x')/P(x(t)))$ where $P(x)$ is the target distribution. The Markov chain is run for many iterations until the chain converges. The samples for which the initial state is forgotten are discarded and known as burn-in samples. The remaining set of accepted values of x represents a sample from the distribution $P(x)$. This algorithm works better when the proposal density matches the shape of the target distribution $P(x)$. Large sample theory states that the posterior distribution of the parameters approaches a multivariate normal distribution therefore a normal proposal distribution is selected often in practice: $Q(x'; x(t)) \sim N(x(t), \Delta^2)$. Here Δ is the step-size and its value is important in obtaining an efficient Markov chain. The search process to find a good parameter value is referred to as tuning. There is no general rule for automatic tuning and off-line tuning may require extensive experimentation.

The MH-algorithm as applied to emitter location estimation problem is presented in Algorithm 1. The algorithm takes the received power values at each sensor and generates samples from the posterior distribution. Here T_{max} shows the number of maximum iterations.

Algorithm 1 M-H algorithm

```
Initialize emitter location, t ← 0
repeat
    Propose a new emitter location S*
    Evaluate η and sample u ∼ U(0,1)
    if u ≤ η then
        Accept the proposed position
    else
        Keep the old position
    end if
    t ← t + 1
until t = T_max
```

The expected a posteriori estimate of the emitter location can be then found by averaging the samples generated by the algorithm. More details about the MH-algorithm can be found in [7].

4. SIMULATIONS

In all simulations in this section, one primary emitter and a number of secondary users were placed in a 1km by 1km square ROI. We assumed independent log-normal shadowing of given dB spread and log-distance path-loss model with a fixed path-loss exponent of 4. The performance results are presented in terms of the root-mean square of the estimation error:

$$RMSE = \sqrt{E(\mathbf{x} - \hat{\mathbf{x}})^2} \quad (1)$$

where $\mathbf{x}$ and $\hat{\mathbf{x}}$ are the actual and the estimated location of the primary emitter.

When an interpolation technique is employed in the simulations, a grid resolution of 10m is assumed.

4.1. Cramer-Rao Lower Bound

The Cramer-Rao lower bound (CRLB) of the localization error for RSS based geo-localization under log-normal shadowing is given by [8]:

$$CRLB = \frac{\ln(10)}{10} \frac{\sigma}{\gamma\sqrt{N}} G \quad (2)$$

where σ and γ are the shadowing spread and the path-loss exponent, respectively, N is he number of sensors and

$$G = \sqrt{\frac{\overline{\tau^2} + \overline{\rho^2} - (\overline{\tau})^2 - (\overline{\rho})^2}{\begin{vmatrix} 1 & \overline{\tau} & \overline{\rho} \\ \overline{\tau} & \overline{\tau^2} & \overline{(\tau\rho)} \\ \overline{\rho} & \overline{(\tau\rho)} & \overline{\rho^2} \end{vmatrix}}} \quad (3)$$

Here, $\overline{\tau}$ and $\overline{\rho}$ are the averages of τ_k and ρ_k, $\overline{\tau^2}$ and $\overline{\rho^2}$ are the averages of τ_k^2 and ρ_k^2, $\tau_k = \frac{\cos(\phi_k)}{d_k}$, $\rho_k = \frac{\sin(\phi_k)}{d_k}$, $\overline{\tau\rho}$ is the average of $\tau_k\rho_k$, and ϕ_k is the angle between the vector emanating from the kth sensor to the emitter and the unit vector
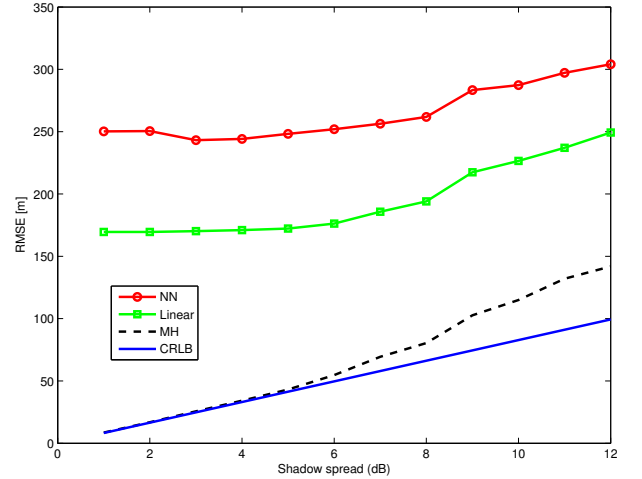

Fig. 1. Comparison of RMSE performances of interpolation and MH-based localization techniques

in the positive direction of the real axis of the reference coordinate system and d_k is the angle and distance between the emitter and kth sensor. Please note that the shadowing spread is assumed to be constant for each emitter-sensor pair. As seen from (2), the CRLB depends on the emitter-sensor geometry, i.e. each unique emitter-sensor placement results in a different CRLB. Therefore a fixed emitter-sensor geometry is used in the simulations where the performance of localization techniques are compared to the CRLB. In one example, we assumed that a primary emitter is located at the centre of the ROI and 16 sensors are placed at the centres of 250 m by 250 m grid locations. The resulting CRLB is plotted in Fig. 1 for shadowing spread values ranging from 1 to 12 dB.

The performances of the NN and linear interpolation based localization techniques are also shown in Fig. 1 for the same emitter-sensor geometry. In these cases the performances at each shadowing spread value were obtained by averaging over 1000 different realizations of the shadowing noise. As seen from these curves, linear interpolation performs slightly better than the NN interpolation based localization; however both techniques perform poorly compared to the CRLB.

Also shown in this figure is the performance of the MH-based localization technique. The performance of the algorithm was calculated using the exact same networks generated in the previous simulations. The step-size of the MH algorithm was set to 200 after a tedious fine tuning stage based on extensive trial and error process. In each simulation, the MH-algorithm was run for 10000 iterations and the first 1000 samples were discarded as burn-in samples. As seen from the figure, MH-algorithm performance is significantly better than the interpolation based localization techniques and its performance is closer to CRLB especially at lower shadow spread values.
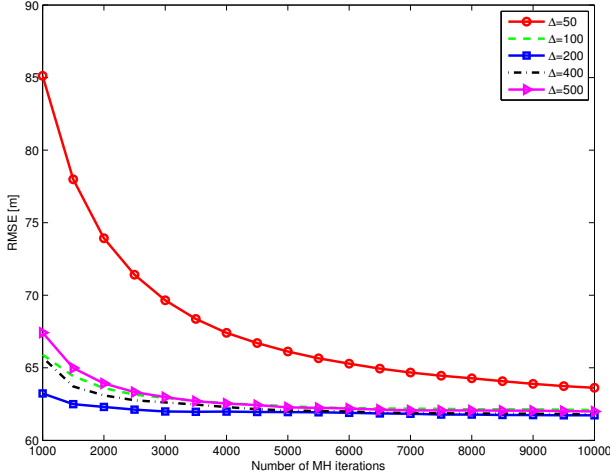
Fig. 2. RMSE performance versus number of MH iterations for different step-sizes

Fig. 3. RMSE performance versus number of burn-in iterations for different step-sizes

4.2. Performance Analysis of MH-Algorithm

As shown in the previous section, the performance of the MH-based localization algorithm is superior compared to the interpolation based localization techniques. However, the performance of the technique is affected by several design parameters such as the selection of the proposal density and its parameters and the numbers of iterations and burn-in samples. Even though the algorithm is guaranteed to converge asymptotically, improper selection of the parameters may slow down the convergence leading to increased computational complexity. Particularly, if the Markov chain is initialized with a value far from the actual emitter location and the step size is small then the chain will require large number of iterations to converge. In order to investigate the effect of parameter selection to the estimation error, we have simulated network scenarios where a primary emitter and 20 sensors are placed randomly chosen locations within the ROI. In these simulations, we evaluated the performance of the MH algorithm in terms of number of burn-in samples and iterations as well as the value of the step-size. Fig. 2 shows the performance as a function of number of MH iterations for different step-sizes. As seen from this figure, the performance is affected by the selection of step-size when the number of iterations is small. The best performance is achieved at $\Delta = 200$. As the number of iterations increases, the performance difference becomes negligible.

Fig. 3 shows the performance of the MH algorithm in terms of the number of burn-in samples for different step-sizes. As seen from these figure, the number of burn-in samples does not affect the performance significantly except when the step-size is set to 50. In this case, at least 2000 burn-in iterations are required for the algorithm to converge.
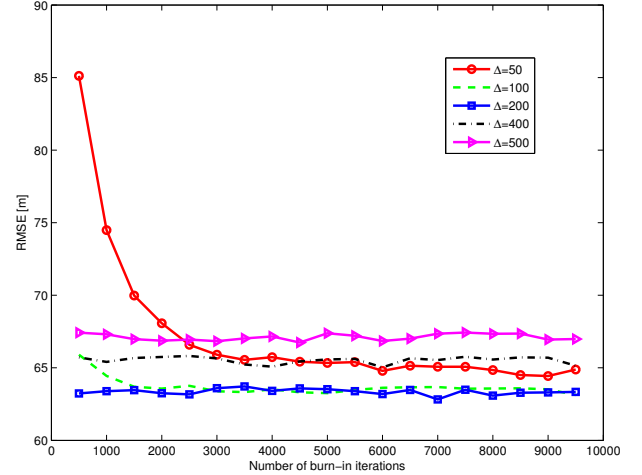
4.3. Comparison of random and smart initializations

In Section 4.2, we have shown that location estimation accuracy of the MH algorithm is affected by the selection of design parameters such as number of burn-in samples and step-size. When these parameters are not set judiciously, the algorithm needs to run a large number of iterations to converge. Our claim is that the required number of MH iteration can be reduced without significant performance loss if the algorithm is jump-started with an initial value obtained from the interference map that the cognitive radio network has already created.

In order to support our claim, we ran simulations to compare performances of random and smart initialized MH-algorithms. In simulations, we randomly deployed secondary nodes and a primary emitter within the ROI. Randomly initialized MH algorithm started at a location chosen arbitrarily within the region whereas the smart algorithm started at the location where the interference map achieved its maximum. Interference maps were created using both NN and linear interpolation techniques. We set the step-size of the proposal density to 50, as this value was resulted in suboptimal performance in simulations performed in Section 4.2. Note that the optimal value of the step-size is not generally available unless the algorithm is tuned-up in advance which requires extensive off-line simulations. The reason for selecting a suboptimal step-size in simulations is due to our desire to compare the performances of both techniques under the worst case scenario. In each simulation, MH algorithm was run for 500 iterations and first 250 samples from these iterations was discarded as burn-in samples. The expected a posteriori estimate of the emitter was then obtained by averaging last 250 samples. The RMS of the location estimation errors were given in Figures 4 and 5. Fig. 4 was obtained by simulating 10000 networks with 30 sensors for each dB spread value ranging from 1 to 12 dB at 1 dB intervals to analyse the performance under shadow fading. Similarly, Fig 5 was obtained by simulating 10000 networks as sensor number was changed
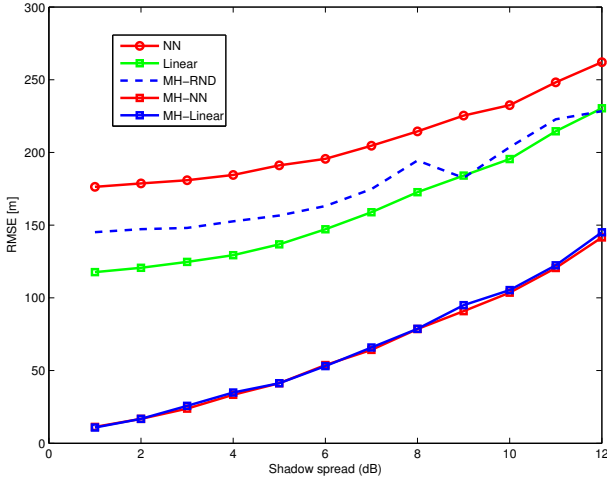
5. CONCLUSIONS

In this paper, we show that localization performance of interference maps obtained using low complexity interpolation techniques are not accurate. Even though the MH algorithm provides more accurate primary emitter location estimates, it takes large number of iterations to converge if its parameters are not tuned in advance. However, when initialized with the knowledge fed-back from the interference map, the MH algorithm converges significantly faster even without parameter tuning.

A natural extension of this study is to consider the case where there are unknown number of multiple primary users with different transmit power levels using reversible jump Markov chain Monte Carlo techniques.

Fig. 4. RMSE performance comparison of localization techniques ($N = 30$)
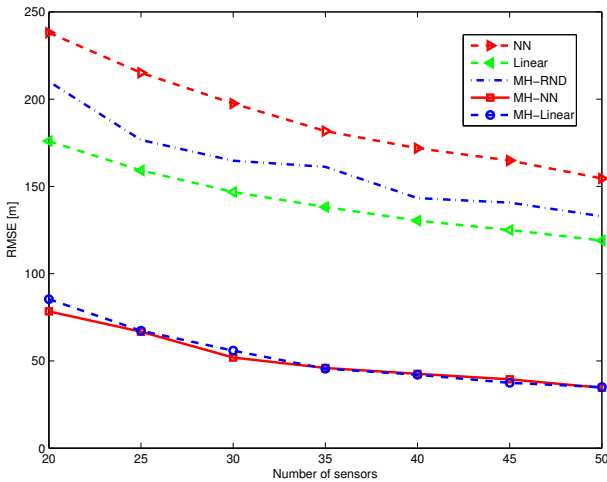

Fig. 5. RMSE performance comparison of localization techniques ($\sigma = 6$)

from 20 to 50. The spread of shadow fading was set to 6 dB in these simulations.

As seen from Figures 4 and 5, randomly initialized MH performs poorly because the algorithm cannot converge due to insufficient number of iterations. In this case, the performance is even worse than the linear interpolation based estimation. When initialized with rough position information provided by the interference map, the MH algorithm achieves significantly better performance even when the number of iterations is small. The performance of the algorithm is the same for both NN and linear interpolation initialization. Even tough the performance of the NN interpolation itself is poorer than the linear interpolation scheme, the performance of the MH is similar for both NN and linear interpolation initialization which shows that the algorithm is insensitive to the accuracy of the initial estimate.

6. REFERENCES

[1] A. Alaya-Feki, S. Ben Jemaa, B. Sayrac, P. Houze, and E. Moulines, "Informed spectrum usage in cognitive radio networks: Interference cartography," in *IEEE PIMRC*, Sept. 2008.

[2] J. Riihijarvi, P. Mahonen, M. Wellens, and M. Gordziel, "Characterization and modelling of spectrum for dynamic spectrum access with spatial statistics and random fields," in *IEEE PIMRC*, Sept. 2008.

[3] S. Grimoud, B. Sayrac, S. Ben Jemaa, and E. Moulines, "An algorithm for fast REM construction," in *Sixth International Conference on Cognitive Radio Oriented Wireless Networks and Communications (CROWNCOM)*, Jun 2011, pp. 251 –255.

[4] S. Ureten, A. Yongacoglu, and E. Petriu, "A comparison of interference cartography generation techniques in cognitive radio networks," in *IEEE ICC*, 2012, pp. 1879–1883.

[5] S. Ureten, A. Yongacoglu, and E. Petriu, "Interference map generation based on delaunay triangulation in cognitive radio networks," in *IEEE SPAWC*, 2012, pp. 134–138.

[6] C. B. Barber, D. P. Dobkin, and H. Huhdanpaa, "The quickhull algorithm for convex hulls," *ACM Transactions on Mathematical Software*, vol. 22, no. 4, pp. 469–483, 1996.

[7] S. Chib and E. Greenberg, "Understanding the Metropolis-Hastings Algorithm," *The American Statistician*, vol. 49, no. 4, pp. 327–335, 1995.

[8] S. Wang, B.R. Jackson, and R.J. Inkol, "Impact of emitter-sensor geometry on accuracy of received signal strength based geolocation," in *IEEE VTC Fall*, 2011.